1

Introduction

1.1 Goals for the Next Linear Collider

For the past 25 years accelerator facilities with colliding beams have been the forefront instruments used to study elementary particle physics at high energies (Figure 1-1). Both hadron-hadron and electron-positron colliders have been used to make important observations and discoveries. Direct observations of the $W^{\pm}$ and Z^{0} bosons at CERN and investigations of the top quark at Fermilab are examples of physics done at hadron colliders. Electron-positron colliders provide well-controlled and well-understood experimental environments in which new phenomena stand out and precise measurements can be made. The discoveries of the charm quark and τ lepton at SPEAR, discovery of the gluon and establishment of QCD at PETRA and PEP, and precision exploration of electroweak phenomena at the SLC and LEP are highlights of the results produced by experiments at electron-positron colliders.

The ability to study nature with these two different kinds of instruments has proven essential to the advancement of our understanding of particle physics. This will remain true as we seek answers to questions posed at the TeV energy scale:

- What is the top quark, and what are its interactions?
- Why is the symmetry of the electroweak interaction broken, and what is the origin of mass?
- Do Higgs particles exist? If so, how many, and what are their structures and interactions?
- Is the world supersymmetric, and if so, what is its structure, and is it part of a larger unification of nature?
- Are quarks, leptons, and gauge bosons fundamental particles, or are they more complex?
- Are there other new particles or interactions, and what might nature contain that we have not yet imagined?

The Large Hadron Collider (LHC) in Europe offers an entry into the TeV energy regime with significant opportunity for discovery of new phenomena. The planned participation in the design, construction, and utilization of this collider by nations around the world will make the LHC the first truly global facility for the study of particle physics. This will be an exciting and important step in the continuing evolution of our science.

The companion electron-positron collider at this next step in energy, a Next Linear Collider (NLC), will provide a complementary program of experiments with unique opportunities for both discovery and precision measurement. To understand the nature of physics at the TeV scale, to see how the new phenomena we expect to find there fit together with the known particles and interactions into a grander picture, both the LHC and an NLC will be required.

Studies of physics goals and requirements for the next-generation electron-positron collider began in 1987-88 in the United States [Ahn 1988, Snowmass 1988, Snowmass 1990], Europe [LaThuile 1987, DESY 1990], and Japan [JLCI 1989, JLCII 1990]. These regional studies have evolved into a series of internationally sponsored and organized workshops [Finland 1991, Hawaii 1993, Japan 1995] that continue to build an important consensus on the goals

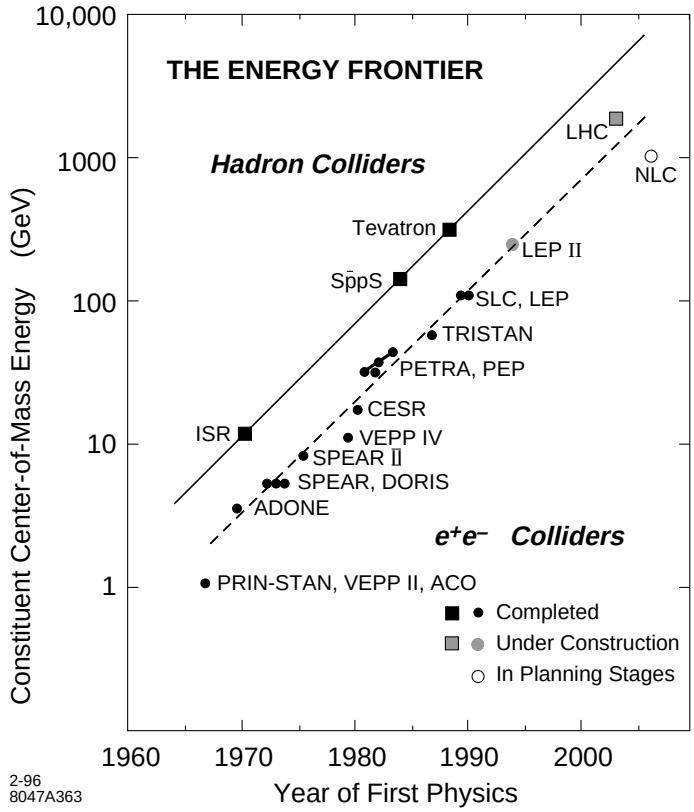

Figure 1-1. *The energy frontier of particle physics. The effective constituent energy of existing and planned colliders and the time of first physics results from each.*

and specifications of a Next Linear Collider. More recently, a series of workshops were held over the past year at locations throughout the United States. Working groups were established at a first meeting in Estes Park, Colorado to provide a framework for people to participate in the discussions of various topics in physics and experimentation at linear colliders. These groups continued to meet at subsequent workshops held at Fermilab, SLAC, and Brookhaven Laboratories. The results of those meetings is presented in a companion document "Physics and Technology of the Next Linear Collider" [NLC Physics] which also provides a summary of the NLC design.

A picture has emerged of a high-performance collider able to explore a broad range of center of mass energies from a few hundred GeV to a TeV and beyond (Figure 1-2). The goals of particle physics at TeV energies require luminosities $\sim 10^{34}\text{cm}^{-2}\text{sec}^{-1}$ and reliable technologies that can provide large integrated data samples. It is important that the beam energy spread remain well controlled and that backgrounds created by lost particles and radiation from the beams be maintained at low levels. This will assure that the clean experimental environment, historically offered by electron-positron colliders, remains intact. Beam polarization, an additional tool available at a linear collider that provides new and revealing views of particle physics, is also a requirement for any future collider.

In this first chapter, we introduce the accelerator physics and technologies of the Next Linear Collider, discuss its design choices and philosophies, and provide a brief status report on the R&D program that is being carried out in support of the NLC design effort. The last section of this chapter will provide an overview of the NLC design and then the design is presented in the following seventeen chapters. This is supplemented with four appendices that describe an alternate power source that might be used for the 1.5 TeV upgrade, a possible second interaction region, ground

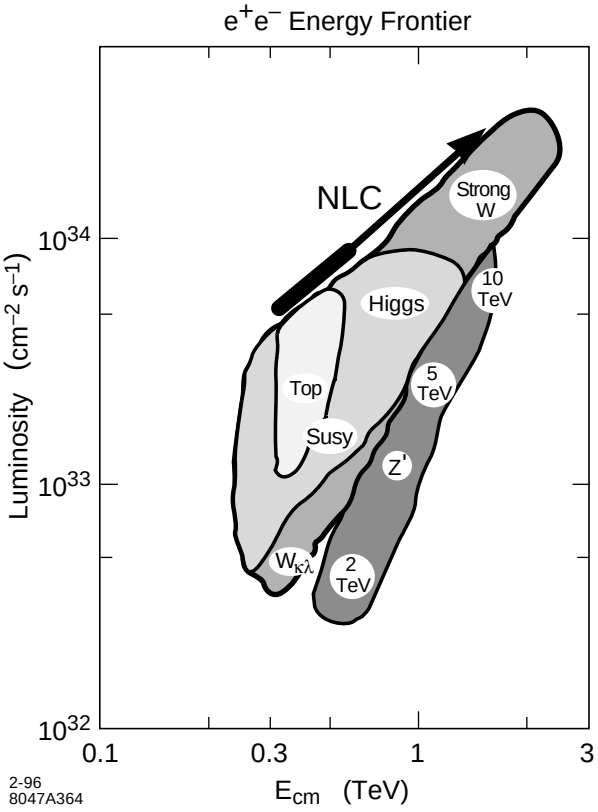

Figure 1-2. *Physics goals for a TeV-scale e^+e^- collider.*

motion studies, and a description of beam-based feedback which is utilized throughout the collider design. As stated, there is also a companion document "Physics and Technology of the Next Linear Collider", that contains results from a series of workshops studying the physics and experimental issues in the NLC as well as a shorter summary of the collider design.

1.2 Accelerator Design Choices

1.2.1 The Stanford Linear Collider

The Stanford Linear Collider (Figure 1-3) was conceived and built to accomplish two goals: to study particle physics at the 100-GeV energy scale and to develop the accelerator physics and technology necessary for the realization of future high-energy colliders. The SLC was completed in 1987 and provided a first look at the physics of the Z^0 in 1989. In time, the luminosity provided by this machine has grown steadily (Figure 1-4), and has allowed particle physicists to make unique and important studies of the Z^0 and its decays.

The design of the Next Linear Collider (NLC) presented in this document is intimately connected with experiences gained at the SLC. Our choices of technologies and philosophies of design have direct links to these experiences and

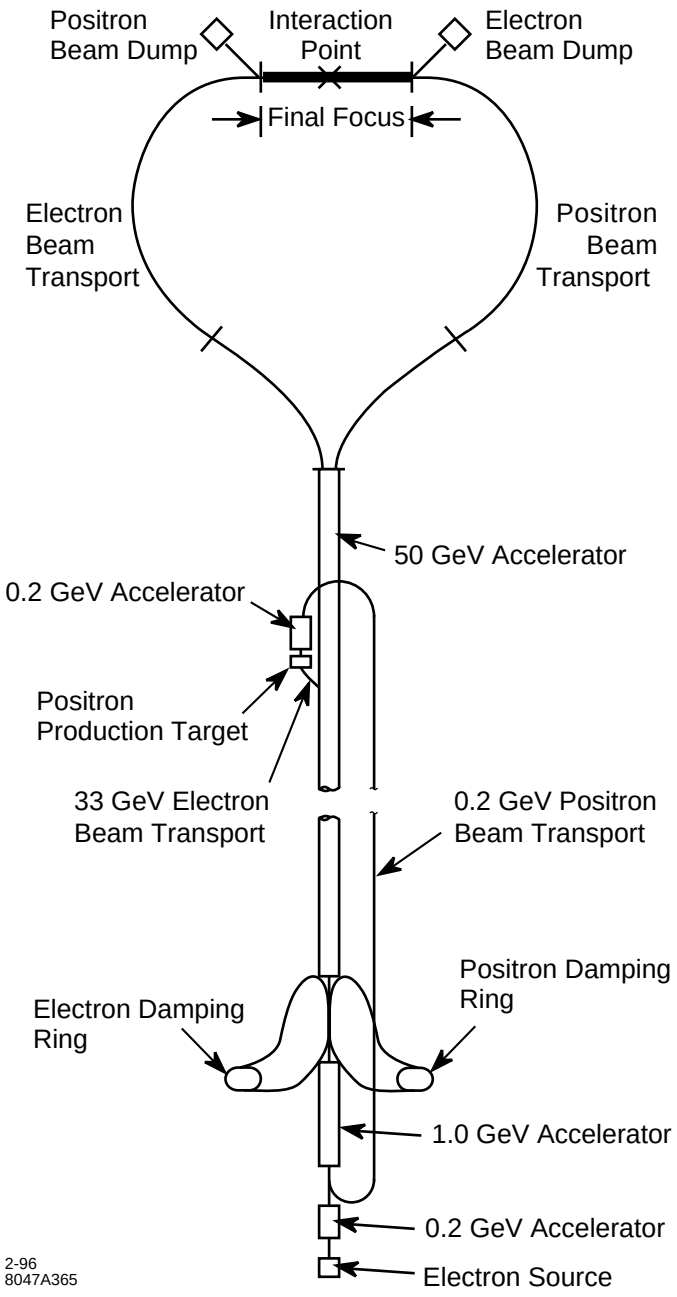

Figure 1-3. *The Stanford Linear Collider (SLC).*

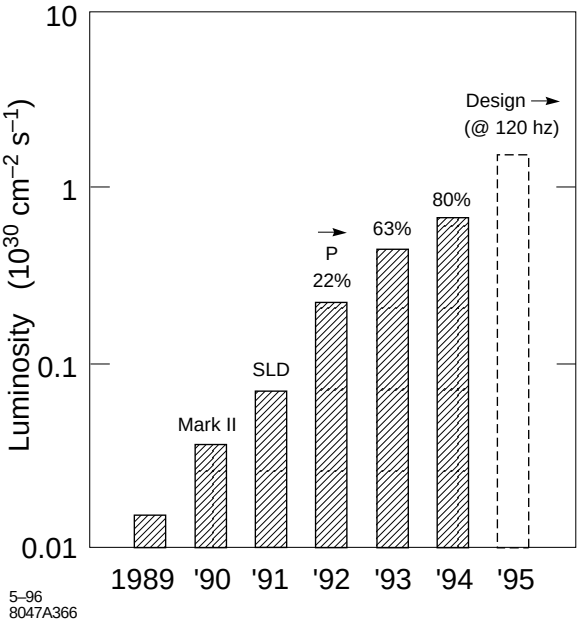

Figure 1-4. *Performance of the SLC from early commissioning. Polarization of the electron beam is also shown.*

considerable overlap with them. Lessons have been learned and techniques developed at the SLC that are relevant to the design and implementation of every part and system of the NLC:

- Injectors
  - Stabilized high-power electron sources
  - Polarized electrons
  - High-power targets and positron capture
- Damping Rings
  - Stabilized fast (50 ns) injection and extraction systems
  - Sub-ps phase synchronization with linac rf systems
- Linear Acceleration
  - Management of large rf systems
  - rf phase control
  - “Time-slot” compensation
  - Short-range longitudinal wake compensation
  - Multibunch beam loading compensation
- Linac Emittance Preservation
  - Beam-based alignment
  - LEM—energy/lattice matching

  - BNS damping
  - Coherent wakefield cancelation
  - Dispersion-free steering
- Final Focus Systems
  - Second-order chromatic optics and tuning
  - Precision diagnostics
  - Beam-beam control and tuning
- Experimentation
  - Theory and modeling of backgrounds
  - Vulnerability of detector technologies
  - Collimation—theory and implementation
- Systems Performance and Operation
  - Precision instrumentation—BPMs and wirescanners
  - Feedback theory and implementation
  - Importance of on-line modeling and analysis
  - Automated diagnostics and tuning
  - Mechanical stabilization of supports and components
  - Thermal stabilization of supports and components
  - Reliability
  - History monitoring (from seconds to years)

1.2.2 Future Linear Colliders

The basic components of any linear collider are those already incorporated into the SLC. The energy of such a future collider must be five to ten times that of the SLC, and a TeV-scale collider must be able to deliver luminosities that are several orders of magnitude greater than those achieved at the SLC. A generic collider complex is diagrammed in Figure 1-5. Trains of bunches of electrons and positrons are created, condensed in damping rings, accelerated to high energy, focused to small spots, and collided to produce a brightness given by

$$L = \frac{nN^2Hf}{4\pi\sigma_x^*\sigma_y^*} \quad , \tag{1.1}$$

where

n = number of bunches per train,
N = number of particles per bunch,
H = L enhancement,
f = machine repetition rate,

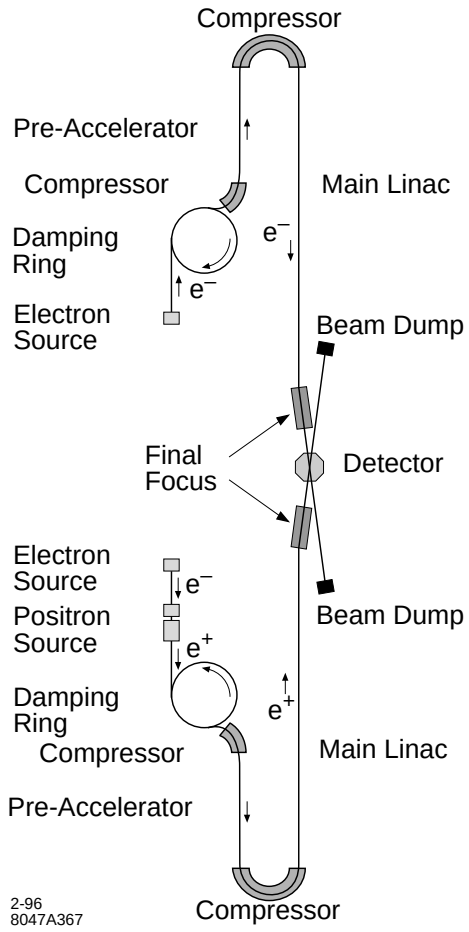

Figure 1-5. *Layout of a TeV-scale linear collider (not to scale).*

and σ_x^* and σ_y^* are the horizontal and vertical beam dimensions at the collision point. Equation 1.1 can be written as

$$L = \frac{1}{4\pi E}\frac{NH}{\sigma_x^*}\frac{P}{\sigma_y^*} \quad , \tag{1.2}$$

where P is the average power in each beam. The factor N/σ_x^* determines the number of beamstrahlung photons emitted during the beam-beam interaction, and since these photons can create backgrounds in experimental detectors, this factor is highly constrained. It is mainly the last ratio that can be addressed by accelerator technology; high luminosity corresponds to high beam power and/or small beam spots. These two parameters pose different, and in many cases contrary, challenges to the accelerator physicist, and several technologies that represent differing degrees of compromise between beam power and spot size are being developed. Table 1-1 summarizes the initial stage of the mainstream design choices.

Each of the technologies in Table 1-1 is being pursued by physicists and engineers at laboratories around the globe. This strong international effort is remarkably well coordinated through collaborations that combine to provide a set of test facilities to address each of the important aspects of the collider design and implementation. A summary of the facilities presently in operation or under construction is given in Table 1-2.

	Rf Freq (GHz)	Rf Grad (MV/m)	Total Length (km)	Beam Power (MW)	σ_y (nm)	Luminosity (10^{33} cm^{-2} s^{-1})
SuperC	1.3	25	30	8.2	19	6
S-Band	3.0	21	30	7.3	15	5
X-Band	11.4	50	16	4.8	5.5	6
2-Beam	30.0	80	9	2.7	7.5	5

Table 1-1. *Linear collider design parameters ($E_{cm} = 500$ GeV).*

Facility	Location	Goal	Operations
SLC	SLAC	Prototype Collider	1988–1998
ATF	KEK	Injector	1995
		Damping Ring	1996
TTF	DESY	SuperC Linac	1997
SBTF	DESY	S-band Linac	1996
NLCTA	SLAC	X-band Linac	1996
CTF	CERN	2-Beam Linac	1996
FFTB	SLAC	Final Focus Interaction Region	1994

Table 1-2. *Linear collider test facilities around the world.*

1.3 The Next Linear Collider

1.3.1 Technology Choice and Design Philosophy

The goal to reach 1 to 1.5-TeV center-of-mass energy with luminosities of 10^{34} cm^{-2} s^{-1} or better and our experiences with the SLC guide our choice of technologies for the NLC. We believe that the most natural match to these design goals is made with normal-conducting X-band (11.424 GHz) microwave components patterned after the S-band technology used in the SLC. A schematic of a section of the rf system for the NLC is shown in Figure 1-6. Our choice of technology has required the development of new rf klystrons and advanced pulse compression systems, but provides confidence that accelerating gradients of 50–100 MV/m can be achieved and used in the implementation of the collider. The technical risk of building a collider with new X-band technologies is perhaps greater than simply building a larger SLC at S-Band, but the goal to reach 1–1.5 TeV is substantially more assured, and capital costs to reach these energies will be lower.

The NLC is designed with a nominal center-of-mass energy of 1 TeV. It is envisaged to be built with an initial rf system able to drive the beams to 0.5-TeV center-of-mass energy, but with all the infrastructure and beam lines able to support 1 TeV. The rf system design incorporates the ability to replace and add modulators and klystrons without access to the accelerator beam line (dashed lines in Figure 1-6), so an unobtrusive, smooth, and adiabatic transition from 0.5 TeV to 1 TeV center-of-mass energy can be made with modest and expected improvements in X-band technology. This allows the collider to begin operation with the greatest of margins in cost and performance, and provides an excellent match

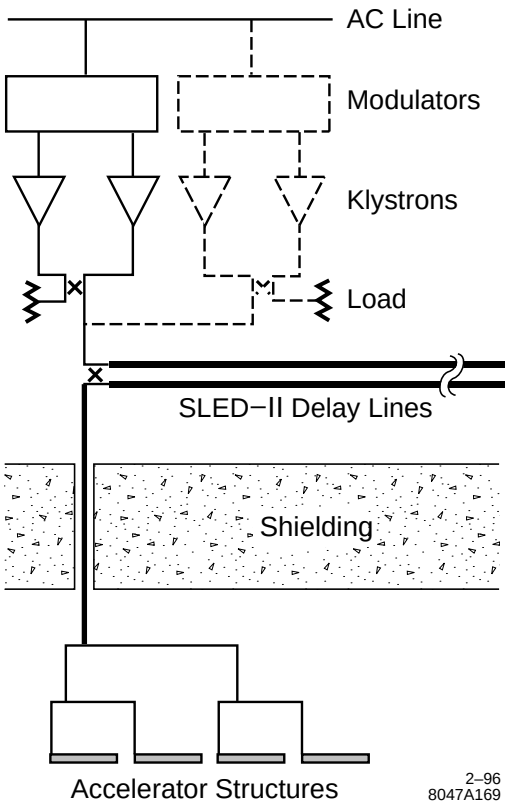

Figure 1-6. *Normal-conducting microwave rf system for the NLC.*

to the anticipated physics goals at the energy frontier (Figure 1-2). Our philosophy is akin to that taken previously in the construction of the SLAC linac which provided a 17-GeV electron beam at its inauguration, was improved to 35 GeV, and with continued advances in S-band technology, now provides 50-GeV electrons and positrons for the SLC.

The NLC design also incorporates multiple paths to further upgrade the center-of-mass energy to 1.5 TeV. The "trombone" shape of the collider layout would easily accommodate a straightforward albeit expensive increase in the length of the main accelerators without requiring extensive modification of the remainder of the complex. This final energy might also be accomplished by development of new, more efficient, X-band technologies; for example, gridded klystrons, cluster klystrons, or relativistic two-beam klystrons.

The highest level parameters of the NLC are listed in Table 1-3. At each of the nominal 0.5 and 1.0-TeV cms energies, three sets of parameters define the operating plane of the collider. The expected luminosity is constant over the operating plane, but is achieved with differing combinations of beam current and spot size. This provides a region in parameter space where the collider can be operated. Construction and operational tolerances for the various subsystems of the collider are set by the portion of the operating plane that is most difficult. For example, the more difficult parameters for the final focus are those of case (a), in which the beam divergences are large. In contrast, preserving the emittance of the beam in the linac is more difficult in case (c), in which the beam charge is highest and the bunch length longest. This design philosophy builds significant margin into the underlying parameters of the collider.

An important element in the design strategy of the NLC is the use of the beam to measure and correct errors in electrical and mechanical parameters of the accelerator. These techniques, many in extensive use at the SLC and FFTB, are able

	NLC-Ia	NLC-Ib	NLC-Ic	NLC-IIa	NLC-IIb	NLC-IIc
Nominal CMS Energy (TeV)		0.5			1.0	
Luminosity w/ IP dilutions (10^{33})	5.8	5.5	6.0	10.2	11.0	10.6
Repetition Rate (Hz)		180			120	
Bunch Charge (10^{10})	0.65	0.75	0.85	0.95	1.10	1.25
Bunches/RF Pulse		90			90	
Bunch Separation (ns)		1.4			1.4	
$\gamma\varepsilon_x$ at IP (10^{-8} m-rad)		400			400	
$\gamma\varepsilon_y$ at IP (10^{-8} m-rad)	7	9	11	9	11	13
β_x/β_y at IP (mm)	8/0.125	10/0.150	10/0.200	10/0.125	12/0.150	16/0.200
σ_x/σ_y at IP (nm)	264/5.1	294/6.3	294/7.8	231/4.4	250/5.1	284/6.5
σ_z at IP (μm)	100	125	150	125	150	150
Υ (Beamstrahlung Param.)	0.10	0.09	0.09	0.33	0.29	0.29
Pinch Enhancement	1.4	1.4	1.5	1.4	1.4	1.5
Beamstrahlung δ_B (%)	3.5	3.2	3.5	12.6	12.6	12.1
# Photons per e^-/e^+	0.97	1.02	1.16	1.65	1.77	1.74
Unloaded Gradient (MV/m)		50			85	
Effective Gradient (MV/m)	31.5	29.4	27.2	58.3	55.1	51.4
Active Linac Length (km)		8.15			8.90	
Min. Total Site Length (km)		23.8			30.5	
Max. Beam Energy (GeV)	267	250	232	529	500	468
Power/Beam (MW)	4.2	4.8	5.5	6.8	7.9	9.0
# of Klystrons		4528			9816	
Klystron Peak Pwr. (MV)		50			72	
Pulse Comp. Gain		3.6			3.6	
RF System Efficiency (%)		28			37	
Total AC Power (MW)		121			193	

Table 1-3. *Present IP and linac parameters of NLC designs.*

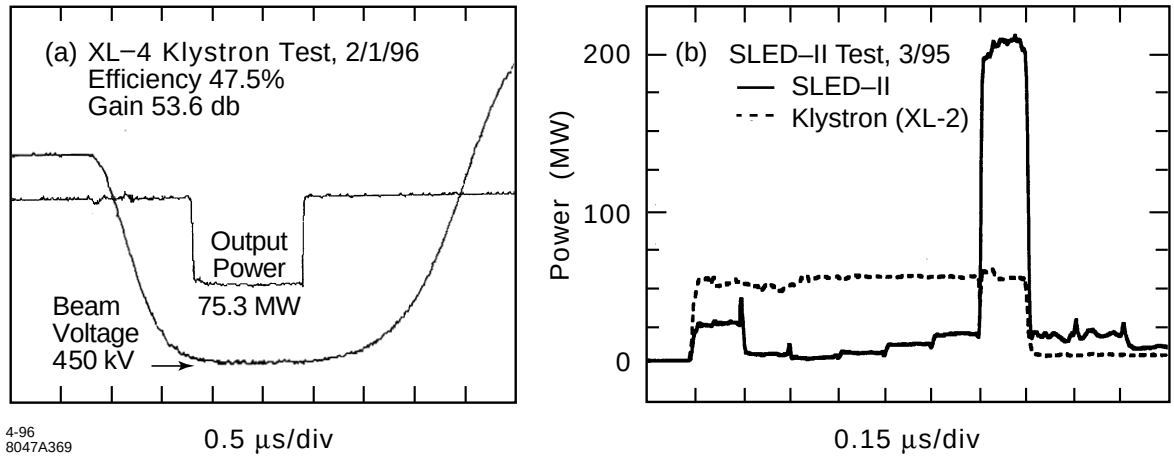

Figure 1-7. *Results of tests of X-band components: (a) high-power klystrons, and (b) rf pulse compression systems.*

to achieve far greater accuracy than is possible during fabrication and installation of components. For example, the use of optical matching and beam-based alignment algorithms considerably loosen tolerances required on magnet strengths and positioning. These procedures require accurate measurement of the properties of the beam and extensive online modeling and software. The existence of instrumentation suitable for these purposes is an important aspect of the readiness of technologies for the collider.

Additional performance overhead has been included in the designs of most subsystems of the NLC and errors that we anticipate occurring during machine tuning and operations have been taken into account. For example, the injector systems, *i.e.*, the particle sources, damping rings, and bunch compressors, are designed to provide 20% more charge than is indicated in Table 1-3 providing a substantial margin over the required performance. Similarly, fabrication and alignment tolerances for the main linac structures are specified without assuming benefit from certain global tuning methods such as coherent wakefield cancelation. These are powerful techniques in routine practice at the SLC, but our philosophy is to use them only to provide operational margin. We also recognize that the beam-based tuning cannot be done with perfect accuracy. For example, we have analyzed the tuning procedure for the final focus and estimated a 30% increase in the spot size at the IP due to errors that we anticipate will occur in measuring and correcting aberrations inherent in the optics. (This is included in Table 1-3.) This layered approach to specification of collider performance is an important part of our design philosophy.

1.3.2 Status Report on Technologies for the NLC

Progress in development of X-band rf components has been impressive in recent years. Prototype klystrons now produce 50 MW, 1.5 μs-long pulses with performance characteristics that are correctly modeled by computer codes. This exceeds the requirements of the initial 0.5-TeV stage of the NLC. In addition, the most recent prototype produces 75 MW, 1.1 μs-long pulses, as required for upgrading the NLC to 1-TeV center-of-mass energy. Tests of pulse-compression transformers have exceeded most goals of the NLC, and high-power rf windows and mode converters that allow high-efficiency transfer of power between components have been successfully tested. Examples of these results are shown in Figure 1-7.

The voltage gradient that can be used in a particle accelerator can be limited by the dark current created when electrons are drawn from the surfaces of the accelerator structures and captured on the accelerating rf wave. For a given rf

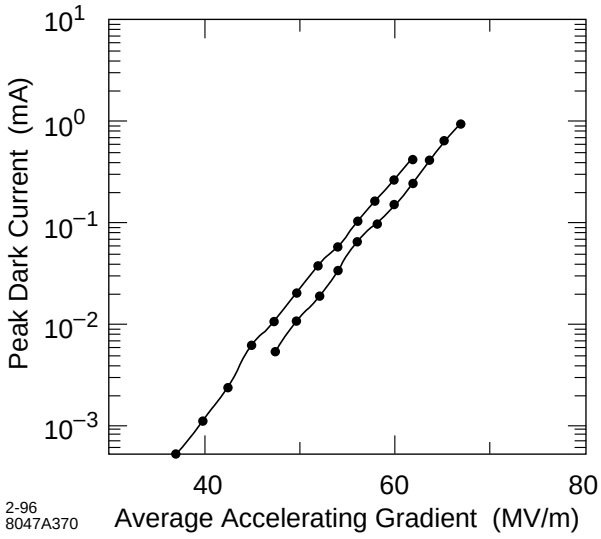

Figure 1-8. *Processing of X-band accelerator structures to high gradient.*

frequency, there is a well-defined gradient beyond which some electrons emitted at rest will be captured and accelerated to relativistic velocities. The capture gradient at S-band is about 16 MV/m, and scales to 64 MV/m at X-band. These are not actual limits to gradients that can be utilized in an accelerator since much of the charge is swept aside by the focusing quadrupoles of the machine lattice, but the dark current will grow rapidly above these values, and may adversely affect the primary beam or interfere with instrumentation needed for tuning. Gradients somewhat above the capture field are likely to be useful in practice, but the operational limits are not well known since no large-scale high-performance facility has been operated significantly above capture gradient. Expected thresholds of dark currents in S-band and X-band structures have been confirmed and it has been shown that (unloaded) gradients as high as 70 MV/m can be attained at X-band (Figure 1-8).

The electro-mechanical design of the main linac accelerator structures must not only produce the desired gradient, but must also minimize wakefields excited by the passage of the beam. The retarded electromagnetic fields left by each particle can disrupt the trajectories of particles that follow it through the accelerator. Many techniques to control the effects of the short distance intrabunch wakefields have been developed, tested, and put into use at the SLC. It will be necessary to also control long-range wakefields at the NLC in order to allow trains of closely spaced bunches to be accelerated on each rf pulse.

Structures that suppress wakefields by careful tuning of their response to the passage of the beam have been developed, and tests have been performed at a facility (ASSET) installed in the SLAC linac (Figure 1-9). Agreement with theoretical expectations is excellent and lends confidence to the design and manufacture of these structures. A more advanced design that further mitigates the long-range wakefields by coupling non-accelerating rf modes to external energy-absorbing materials has been completed, and a prototype of this new structure is being readied for testing in ASSET as well.

Work remains to be done on X-band rf technologies, but with prototype components now in hand, tests of completely integrated systems have begun. A fully engineered accelerator is under construction at SLAC that will allow optimization of rf systems and provide experience with beam operations at X-band frequencies. This test accelerator will be a 40-m-long section of six, 1.8 m X-band structures powered by 50–75 MW klystrons to an accelerating gradient of 50-85 MV/m. Commissioning of this facility has begun, and operations are expected to be under way by the end of this year (Table 1-2).

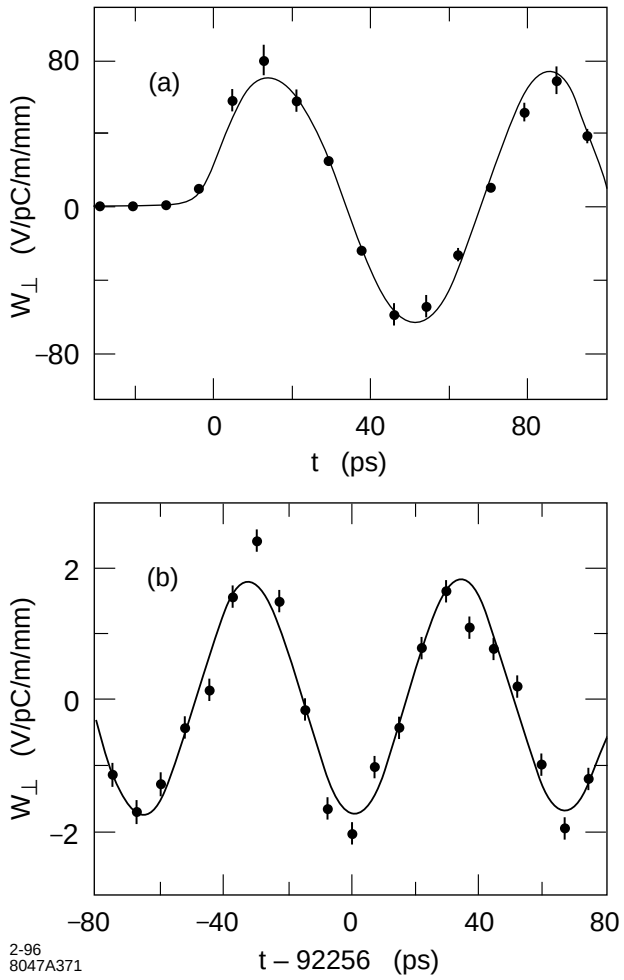

Figure 1-9. *Measured (circles) and predicted (line) transverse dipole wakefields in a 1.8-m-long X-band accelerator structure where (a) shows the wakefield immediately following a bunch and (b) shows the wakefield 92 ns later; note the large decrease in amplitude.*

The spot sizes that must be produced at the interaction point of the NLC represent significant extrapolations from those achieved at the SLC. It is important to demonstrate that it is possible to demagnify a beam by the large factor needed in the NLC. An experiment has been performed by the Final Focus Test Beam Collaboration to show that such large demagnifications can be achieved. The Final Focus Test Beam (FFTB) is a prototype beam line installed in a channel located at the end of the SLAC linac at zero degrees extraction angle. The FFTB lattice is designed to produce a focal point at which the beam height can be demagnified by a factor of 380 to reduce the SLC beam ($\gamma\varepsilon_y = 2 \times 10^{-6}$ m-rad) to a size smaller than 100 nm. The demagnification factor of the FFTB beam line is well in excess of that needed for the NLC.

The FFTB optics are chromatically corrected to third-order in the beam energy spread. (The SLC is corrected to second order.) All magnetic elements are mounted on precision stages that can be remotely positioned with step size of ≈ 0.3 micron, and beam-based alignment procedures were developed that successfully place these elements to within 5–15 microns of an ideal smooth trajectory. New state-of-the-art instruments were developed and used to measure the FFTB beam positions and spot sizes. Following a brief shake-down run in August of 1993, data were taken with the FFTB

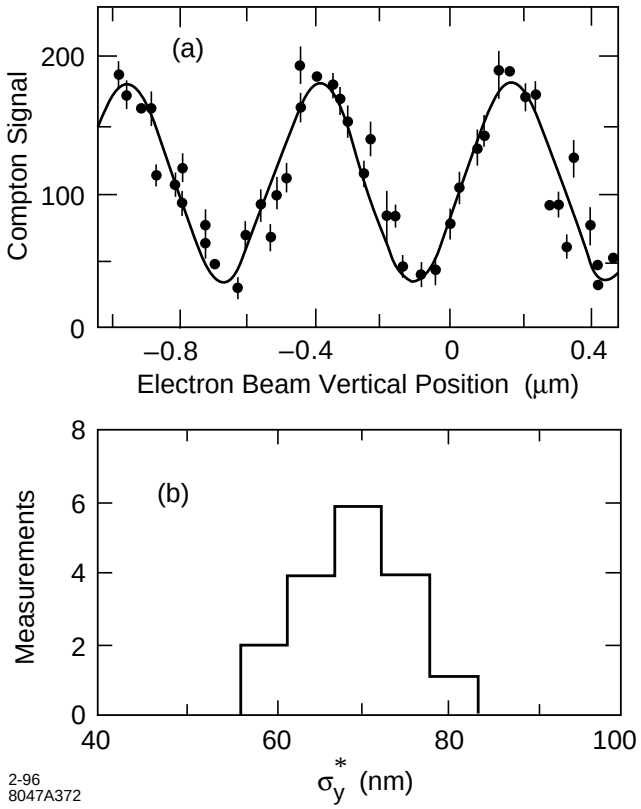

Figure 1-10. *Measurement of 70-nm beam spots with a laser-Compton beam size monitor in the FFTB. (a) The rate of Compton scatters from a laser interference pattern used to determine the beam size, in this case 73 nm. (b) Repeatability of spot measurement over periods of several hours.*

during a three-week period in April and May of 1994. Beam demagnifications of 320 and spot sizes of 70 nm were controllably produced during this period. Measurement of these beams is shown in Figure 1-10. The design of the NLC final focus follows that of the FFTB, and the experiences gained from the FFTB are incorporated into the tuning strategies of the NLC.

Important advances have also been made in instrumentation required to measure and control properties of the beam. The SLC control system has evolved dramatically over the past years to include extensive online modeling and automation of data analysis and tuning procedures. Scheduled procedures use sets of wire scanners to make complete measurements of the beam phase space, and provide recorded histories of machine performance. Online data analysis packages are able to reconstruct fully coupled non-linear optical systems. Beam-based feedback and feedforward are in routine operation in the SLC with over 100 loops providing control of beam trajectories and energies. Beam position monitors have been developed for the FFTB that achieve pulse-to-pulse resolutions of 1 micron, and new position monitors have recently been installed that are able to measure beam motions of 100 nm. The FFTB focal point spot monitors have demonstrated techniques to measure beam sizes of 30–40 nm, and extrapolation of these techniques to sizes as small as 10 nm can be expected to be successful.

1.4 Outlook for the Next Linear Collider

As the SLC has systematically increased its luminosity, the accelerator physics and technologies of linear colliders has matured. Experiences and lessons learned from the task of making this first collider perform as an instrument for particle physics studies make a firm foundation on which to base the design and technology choices for the next linear collider. At the same time, the essential demonstrations of new collider technologies have either taken place or soon will be underway. The experimental program with the FFTB is providing the experience needed to evaluate limitations to designs of final focus and interaction regions. The ability to demagnify beams by the amount required for the NLC has already been achieved. Microwave rf power sources have exceeded requirements for the initial stage of the NLC and critical tests assure us that this technology can be expected to drive beams to center-of-mass energies of a TeV or more. Fully integrated test accelerators are presently under construction at CERN, DESY, KEK, and SLAC that will soon provide answers to questions of technical optimization and costs of the major components of a TeV-scale collider.

Given the great international interest and commitment to the goals of a TeV-scale high-performance e^+e^- collider, it is certain that its final design, construction, and utilization will be a global effort. It is important that the scientific community put into place foundations for such a collaboration. The international character of the linear collider project is already reflected in the collaborations at work on the accelerator physics and technology of linear colliders and in the process of international discussion and review of progress in the field [Loew 1995]. It is essential that we continue to build on this base of understanding and cooperation and make certain that all involved in this enterprise are full party to its final realization.

1.5 NLC Systems Overview

The Next Linear Collider consists of a set of subsystems—injectors, linacs, beam delivery, and interaction regions. These are responsible for creating intense and highly condensed beams of positrons and polarized electrons, accelerating them to high energy, focusing them to small spots, and colliding them in an environment that allows sensitive particle detectors to operate for physics. In this section, we introduce these various parts of the collider while pointing to the more detailed discussions in the following text. We will also describe the energy upgrade and other more global issues.

A schematic of the NLC is shown in Figure 1-11. The physical footprint of the collider complex is approximately 30 km in length and less than 1 km wide. This includes all beam transport lines in the injectors and linacs necessary to obtain 1 TeV center-of-mass energy, and all space need in the beam delivery sections to accommodate 1.5 TeV center-of-mass energy. To reach 1.5 TeV, however, it may be necessary to extend the “trombone” layout of the collider to provide additional length for the linac. This can be done without moving the injectors or damping rings.

Injectors

The injector systems prepare the beams for injection into the main linacs at a beam energy of 10 GeV. The injectors consist of the polarized electron and positron sources, the damping rings, which reduce the transverse emittances of the beams, and the bunch compressors, which reduce the bunch lengths. Because they must provide a stable and reliable platform for the rest of the linear collider, we have been careful to design the systems with substantial operating margin.

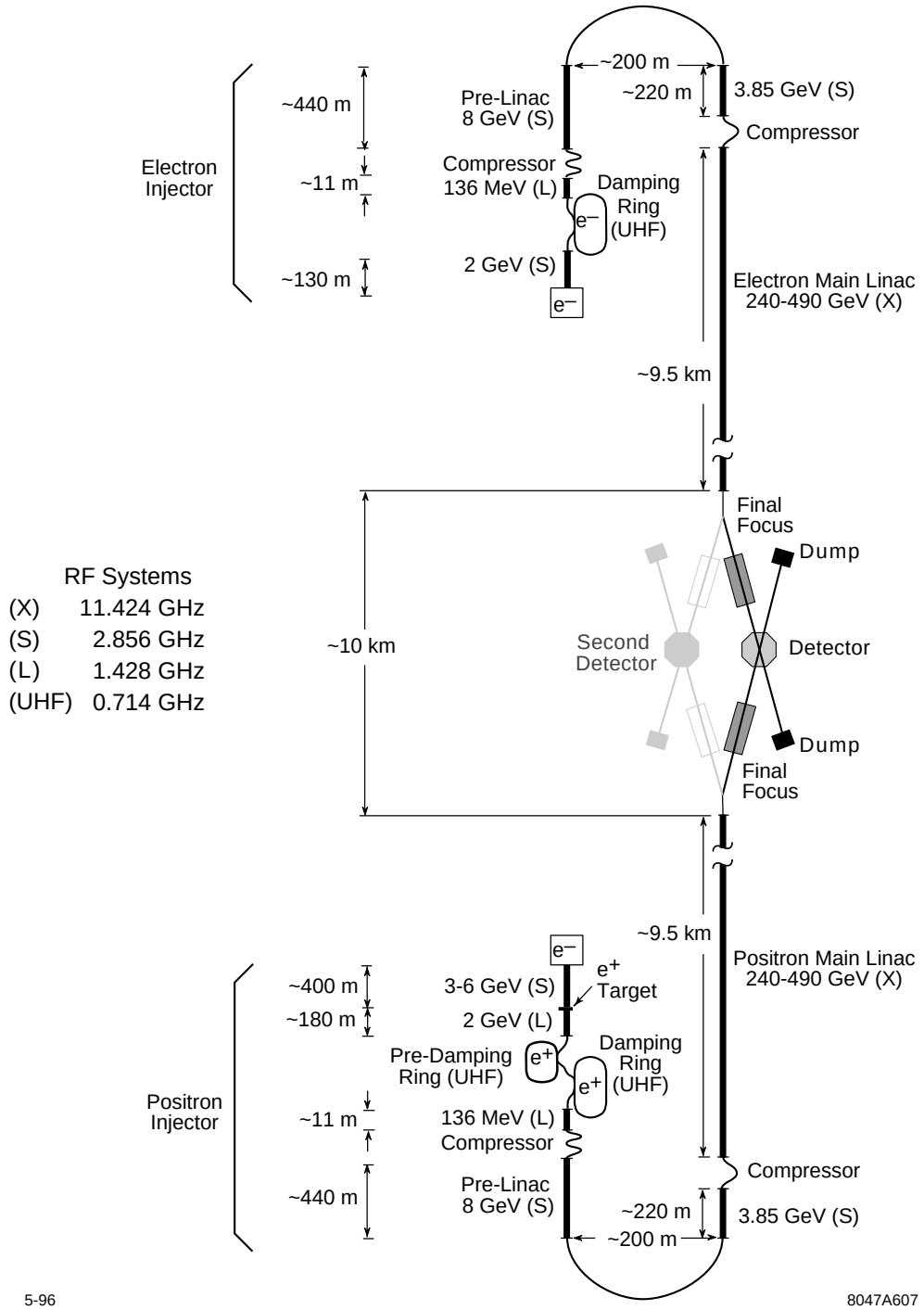

Figure 1-11. *Schematic layout of NLC systems (not to scale).*

The polarized electron source (Chapter 2) for the NLC is copied from the present SLC system which generates beams with $> 75\%$ polarization and operates very reliably. The NLC source includes a polarized laser, a photocathode electron gun, and a non-relativistic subharmonic bunching system. The new challenge for the NLC source is that it must produce trains of 90 bunches spaced by 1.4 ns at the machine repetition rate of 120–180 Hz. This is done by modulating a 126-ns laser pulse with a series of resonant rf Pockels cells. To get a relatively rectangular intensity profile, the modulation is performed using the first and third harmonic of the bunch spacing.

The bunched beam from the electron source is accelerated in an S-band (2.856 GHz) booster linac to 2 GeV and then injected into a damping ring (Chapter 4). The damping ring stores four trains of 90 bunches at once, extracting the oldest train as a new one is injected. It is designed to damp the transverse phase space of the beam from the incoming normalized emittances of $\gamma\epsilon_{x,y} = 1 \times 10^{-4}$ m-rad to $\gamma\varepsilon_x = 3 \times 10^{-6}$m-rad and $\gamma\varepsilon_y = 3 \times 10^{-8}$m-rad. These damped horizontal and vertical emittances are much smaller than those achieved in the SLC damping rings, and are comparable to those in the present generation of synchrotron light sources such as the Advanced Light Source at Lawrence Berkeley National Laboratory. To attain the small emittances, the ring is designed with a strong focusing lattice and uses beam-based techniques to achieve the required alignment of the ring magnets. The damping ring design incorporates lessons and techniques learned from operation of the SLC as well as experiences from the more modern synchrotron light sources. Finally, many of the components required in the rings have already been or soon will be designed and tested in other storage rings. This includes the wiggler magnets, which are included in the NLC design to reduce damping times, multibunch feedback and rf systems, and the vacuum system.

The technique for production of positrons that is planned for the NLC (Chapter 3) is also largely copied from that used at the SLC. Here, positrons are created in electromagnetic showers produced by targeting a 3–6 GeV electron bunch train onto a rotating $W_{75}Re_{25}$ target; the 3–6 GeV electron beam is produced with a conventional thermionic electron source and accelerated in a separate S-band linac. The large emittance positron beam is captured and accelerated to 2 GeV in a large-aperture L-band (1.428 GHz) linac. This lower frequency rf system has a smaller beam loading and leads to a good capture efficiency because of the increased longitudinal and transverse apertures.

At the 2-GeV point, the positron beam, with transverse emittances of 0.06 m-rad, is cycled through a large-aperture pre-damping ring (Chapter 4). The pre-damping ring damps the incoming positron emittances to $\gamma\epsilon_{x,y} = 1 \times 10^{-4}$ m-rad prior to injection into a main ring which is identical to that used for the polarized electron beam. Finally, the overall layout also includes transport lines that will allow the drive electron beam to bypass the positron production target and pre-damping ring to allow the study of e^-e^- or $\gamma\gamma$ collisions (with both electron or photon beams polarized).

Next, the lengths of the electron and positron bunches become too great in the damping rings for the beams to be successfully accelerated in the main X-band linacs, so they must be reduced (Chapter 5). This is done in two stages. A first bunch compressor, located immediately after the damping rings, reduces the bunch length from 4 mm to 500 μm to optimize injection into an S-band linac that accelerates the beams to 10 GeV. The bunch lengths are then further compressed to 100–150 μm in a compressor that rotates the longitudinal phase space by 360° and reverses the direction of travel; this arc allows for future upgrades of the main linac length and permits feedforward of the bunch charge and trajectory made in the damping rings and compressors.

Finally, the rf acceleration throughout the injector systems, *i.e.*, the bunch compressor rf, the 8-GeV prelinacs, and the 2-GeV booster linacs, is performed with relatively low frequency rf. In particular, the positron booster linac and the first bunch compressors operate at L-band (1.4 GHz) and the electron booster linac, the prelinacs, and the second bunch compressor operate at S-band (2.8 GHz). Although these systems are, in general, longer and more expensive than higher frequency accelerator systems, we feel that they are needed at the lower beam energy. In particular, we have designed the systems so that they have small beam loading and relatively loose alignment tolerances. This is important to provide the reliability and stability that is desired in the injector systems. Of course, such lightly-loaded systems are inefficient and could not be used to accelerate the beams to very high energy.

To minimize the long-range transverse wakefields, all of the accelerator structures are damped and detuned structures, similar to those developed for the X-band main linacs. In addition, the beam loading is primarily compensated using the ΔT (early injection) method which is discussed in Chapter 6. This has the advantage of canceling the bunch-to-bunch energy deviations locally within an accelerator structure thereby minimizing the transverse emittance growth due to dispersive and chromatic effects. Details of the multibunch beam loading compensation in the injector linacs as well as the low frequency accelerator structures and power sources is presented in Chapter 6.

Main Linacs

The main linacs of the NLC use normal-conducting traveling-wave copper structures operating at X-band (11.424 GHz). The choice of such a high frequency, relative to existing high-energy linacs, allows higher accelerating gradient, shorter linac length, and lower AC power consumption for a given beam energy. Considering the size, weight, cost, and availability of standard microwave components, we have chosen a frequency in the X-band for a design that is upgradeable from an initial 500-GeV center-of-mass energy to 1 TeV or more.

In the 500-GeV center-of-mass design, the required rf power is generated by 50 MW klystrons in 1.2 μs pulses which is then compressed to 0.24 μs, with higher peak power, by a passive rf transformer (SLED-II); this provides an unloaded acceleration gradient of 50 MeV/m. The upgrade to 1-TeV center-of-mass energy is accomplished by doubling the number of modulators and by replacing each 50-MW klystron with a pair of 75-MW klystrons. This attains an unloaded gradient of 85 MV/m. To achieve the full 1-TeV center-of-mass design, the total active length of linac must be increased slightly from 16,300 m to 17,700 m. This would be done by replacing spool pieces at the ends of the linac beam lines with accelerator structures. In addition, the planned upgrade includes improvements in the modulator and pulse compression systems to increase the rf system efficiency. The rf system for both the 500-GeV design and the 1-TeV upgrade is described in Chapter 8.

The rf system operates with a repetition frequency of 120–180 Hz. On each rf pulse, a train of 90 bunches is accelerated in each linac. While the number of particles in each of these bunches is small compared to that in the SLC, the total charge accelerated by each rf pulse is more than an order of magnitude greater. This multibunch design and the correspondingly larger fraction of energy transferred from the power sources to the beam is one of the important differences between the SLC and the NLC.

Extensive effort has been made on the design of an accelerator structure and rf system to ensure that both the beam loading can be compensated to the level required and the long-range transverse wakefield does not significantly increase the transverse emittances. The beam loading is compensated by optimizing the temporal profile of the rf pulse by shifting the phase of the rf from the klystrons. The long-range transverse wakefields have been reduced by tailoring the cell-to-cell dipole mode frequency to yield a Gaussian-like decay of the wakefield and by coupling each of the cells to four damping manifolds; this accelerator structure is referred to as a Damped-Detuned Structure (DDS). The technical designs of these rf components are described in Chapter 8 while many of the issues associated with the multibunch operation are summarized in Chapter 13.

The design and layouts of the linacs and the beam dynamics studies are presented in Chapter 7. The focusing lattice of the linac is designed to allow the center-of-mass energy to vary from 300 GeV to 1 TeV. Thus it does not have to be modified for the 1-TeV upgrade; the upgrade to 1.5-TeV will require changes. To verify the state of the beam, five diagnostic stations, located along each of the two main linacs, will include laser wire scanners to measure the transverse phase space, beam-based feedbacks to correct for centroid shifts of the bunch train, multibunch BPMs and high-frequency kickers to measure and correct bunch-to-bunch position errors, and magnetic chicanes to provide non-invasive energy and energy spread measurements.

The components in the linacs will have to be aligned to a few microns of a tuned reference orbit to prevent excessive emittance growth. This will be done using beam-based alignment techniques and high resolution beam position

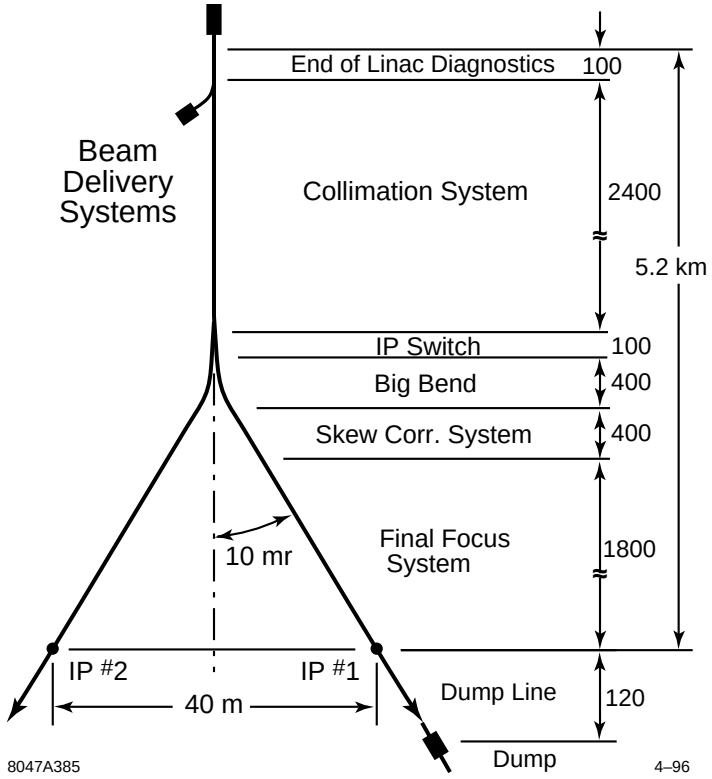

Figure 1-12. *Schematic layout of the beam delivery system.*

monitors. Studies of vibration and stability, based on measurements of the ground motion made at SLAC and described in Appendix C, show that the linac is not extremely sensitive to the motion. Fast feedback systems, similar to those used at the SLC and described in Appendix D, are required to stabilize the beam and the trajectories will need to be re-steered every 30 minutes; neither of these presents an operational limitation.

The Beam Delivery System

The beam delivery system consists of a collimation section, a switchyard, the final focus, the interaction region, and the beam extraction and dump. These are shown schematically in Figure 1-12. The overall lengths of the beam lines have been designed to allow for a final beam energy of 750 GeV.

After acceleration in the main linacs, the beams enter the collimation sections, described in Chapter 9, where particles at the extremities of the energy and transverse phase space are eliminated. The collimation is performed in both the horizontal and vertical planes at two betatron phases that differ by 90° to effectively cut the beam in both position and angle. This primary collimation is then followed by a secondary collimation in both planes and both phases to remove particles that are scattered by the edges of the primary collimators. The collimation regions have been designed to absorb 1% of the nominal beam power while surviving the impact of a full bunch train. The system consists of a series of spoilers and absorbers which have been optimized to reduce the transverse geometric and resistive-wall wakefields. Although the collimation sections are rather extensive, our experiences at the SLC and Final Focus Test Beam (FFTB) have proved the need to perform this function very carefully.

The collimation regions are followed by passive switching sections (Chapter 10) which are used to direct the beams to one of two possible interaction points (IPs). The beams are each deflected in the switchyard by 10 mr to produce a net 20-mr crossing angle at the IPs. This deflection introduces only little emittance growth, but greatly reduces detector backgrounds and provides the IP crossing angle required to collide the closely spaced bunches in each train.

The NLC final focus is described in Chapter 11. It follows the design of the FFTB at SLAC. The optics consist of a matching section with appropriate instrumentation to measure the incoming beam phase space, horizontal and vertical chromatic correction sections, a final transformer, a final doublet, and a diagnostic dump line for the exiting beam. The final focus system is chromatically corrected to third order. It demagnifies the transverse beam sizes by a factor of 80 horizontally and 300 vertically. A dedicated geometry adjustment section is included to facilitate the adiabatic upgrade from 350 GeV to 1.5 TeV center-of-mass without changing the IP position and requiring only minor transverse realignment of the beam line.

Although there is less demagnification than in the FFTB, the vertical spot size at the IP is roughly 15 times smaller than that attained in the FFTB. This imposes stringent tolerances which are achieved using beam-based tuning techniques and feedback systems. Measurement of the final spot size is a particular challenge, but can be performed with an advanced laser fringe monitor similar to that used in the FFTB and in-situ tuning of the spot sizes and luminosity can be done using measurements of the beam-beam deflections and techniques developed at the SLC. An extensive accounting of all the aberrations and the limitations of the tuning methods, including the different time scales required and the measurement accuracy, has been included in the luminosity calculations; these amount to a reduction in luminosity of 30–40%.

Interaction Region

Two interaction regions (IRs) are included in the layout of the NLC. The two important issues for the NLC IRs are the backgrounds and masking and the vibration stabilization of the final doublet; these are discussed in Chapter 12. The two IRs, of course, must share the available luminosity, but it will be possible to install two complementary experiments. As with all colliders, the interaction region will be a very crowded location. The final quadrupole magnets of the machine optics must be positioned as closely as possible to the collision point, and high-Z masking must be installed to protect elements of the experimental detector. The detector itself will require clear access to as much of the volume around the interaction point as possible. The design presented in this document includes quadrupoles two meters from the interaction point, and complete access for detector elements at polar angles greater than 150 mr. Calorimetric measurement of Bhabha scatters at smaller polar angles should also be possible, and are expected to provide precise determination of the luminosity-weighted center-of-mass energy spectrum.

The NLC is designed to collide electrons and positrons beams at a small (20 mr) crossing angle. This prevents the tightly spaced bunches of one beam from being disturbed as they approach the interaction point by bunches in the opposing beam that are leaving the interaction point. To avoid loss of luminosity due to this crossing angle, it is necessary to use a pair of small deflecting-mode rf cavities to “crab” the beams so that the bunches collide head-on. This is a new task not encountered at the SLC, but a system with reasonable specifications has been designed.

Global Considerations

Finally, the last five chapters discuss more global issues in the collider. As mentioned, the NLC will operate with long trains of bunches. Multibunch operation is one of the major differences between the NLC and the SLC. The issues associated with the multibunch operation are covered throughout the text but, because it is an important topic, we summarize these issues in Chapter 13.

Next, the control system and the instrumentation issues are outlined in Chapters 14 and 15. With the heavy utilization of beam-based alignment and tuning, the control system and the instrumentation design are very important for the NLC. The control system design uses many lessons learned from the SLC control system which has evolved substantially to meet the SLC requirements. Similarly, much of the required instrumentation is based on designs that have already been demonstrated. In the future, we will organize the description of the instrumentation into a unifying chapter but, at this time, the design and requirements are described throughout the text. Chapter 15 provides a short introduction to the philosophy of the instrumentation design and utilization.

The Machine Protection System (MPS) is described in the next chapter, Chapter 16. Because of the very high beam density and large beam power, the MPS is a difficult system and imposes significant constraints on the operation of the collider.

Finally, the NLC is a large and complex instrument and reliability is very important consideration. The SLC operates with an overall accelerator availability of roughly 80% and the NLC will be roughly ten times larger. Simple scaling of the SLC fault rates would suggest that the NLC would be effectively inoperable. Reliability considerations need to be addressed in the design from the onset and they are discussed in Chapter 17.

Lastly, the facilities and conventional systems for the NLC are described in Chapter 18. This includes the power and cooling distribution, the accelerator housing and the klystron gallery, as well as the campus and support facilities.

Appendices

In addition to the main body of the text, four appendices are included in this document. Appendices A and B present a possible rf system for a 1.5-TeV center-of-mass upgrade which is based on a Two-Beam Accelerator and a design for an interaction region to produce and study $\gamma\gamma$ collisions. These are followed by Appendices C and D which discusses ground motion theory and measurements and the implementation and limitations of beam-based feedback.

References

[Ahn 1988] C. Ahn, *et al.*, SLAC–Report–329, 1988.

[CERN 1987] Proceedings of the Workshop on Physics at Future Accelerators (La Thuile), CERN, Geneva, 1987.

[Snowmass 1988] Proceedings of the 1988 DPF Summer Study: Snowmass '88, High Energy Physics in the 1990s, E.L. Berger, ed., Snowmass, CO, 1988.

[JLCI 1989] Proceedings of the First Workshop on Japan Linear Collider (JLC I), S.Kawabata, ed., KEK, 1989.

[Snowmass 1990] Proceedings of the 1990 DPF Summer Study on High Energy Physics: Research Directions for the Decade, F. Gilman, ed., (Snowmass, CO, 1990).

[JLCII 1990] Proceedings of the Second Workshop on Japan Linear Collider (JLC II), (KEK, 1990).

[DESY 1990] Workshop on Electron-Positron Collisions at 500 GeV: The Physics Potential, (DESY, 1990).

[Finland 1991] Proceedings of the First International Workshop on Physics and Experiments with Linear Colliders, R. Orava, ed., (Saariselka, Finland, 1991).

[Hawaii 1993] Proceedings of the Second International Workshop on Physics and Experiments with Linear Colliders, F. Harris, et al., eds., (Waikoloa, Hawaii, 1993).

[Japan 1995] Proceedings of the Third International Workshop on Physics and Experiments with Linear Colliders, (Iwate, Japan, 1995).

[LaThuile 1987] Proceedings of the 1987 LaThuile Meeting: Results and Perspectives in Particle Physics, M. Greco, ed., (Gif-sur-Yvette, France, 1987).

[NLC Physics] "Physics and Technology of the Next Linear Collider: A Report Submitted to Snowmass 1996", SLAC Report–485; BNL–52–502; Fermilab–Pub–96/112; LBNL–Pub–5425; UCRL–ID–124160.

[Loew 1995] G. Loew, et al., International Linear Collider Technical Review Committee Report, SLAC Report–471 (1996).